

Fabrication and performance evaluation of GaN thermal neutron detectors with ^{6}LiF conversion layer

Zhifu Zhu(朱志甫), Zhijia Sun(孙志嘉), Jijun Zou(邹继军), Bin Tang(唐彬), Qinglei Xiu(修青磊), Renbo Wang(王仁波), Jinhui Qu(瞿金辉), Wenjuan Deng(邓文娟), Shaotang Wang(王少堂), Junbo Peng(彭俊波), Zhidong Wang(王志栋), Bin Tang(汤彬), Haiping Zhang(张海平)

Citation: Chin. Phys. B . 2020, 29(9): 090401 . **doi:** 10.1088/1674-1056/ab9c05
Journal homepage: http://cpb.iphy.ac.cn; http://iopscience.iop.org/cpb

What follows is a list of articles you may be interested in

Comparative study on characteristics of Si-based AlGaN/GaN recessed MIS-HEMTs with HfO_2 and Al_2O_3 gate insulators

Yao-Peng Zhao(赵垚澎), Chong Wang(王冲), Xue-Feng Zheng(郑雪峰), Xiao-Hua Ma(马晓华), Kai Liu(刘凯), Ang Li(李昂), Yun-Long He(何云龙), Yue Hao(郝跃)
Chin. Phys. B . 2020, 29(8): 087304 . **doi:** 10.1088/1674-1056/ab8daa

Trap analysis of composite 2D-3D channel in AlGaN/GaN/graded-AlGaN: Si/GaN: C multi-heterostructure at different temperatures

Sheng Hu(胡晟), Ling Yang(杨凌), Min-Han Mi(宓珉瀚), Bin Hou(侯斌), Sheng Liu(刘晟), Meng Zhang(张濛), Mei Wu(武玫), Qing Zhu(朱青), Sheng Wu(武盛), Yang Lu(卢阳), Jie-Jie Zhu(祝杰杰), Xiao-Wei Zhou(周小伟), Ling Lv(吕玲), Xiao-Hua Ma(马晓华), Yue Hao(郝跃)
Chin. Phys. B . 2020, 29(8): 087305 . **doi:** 10.1088/1674-1056/ab96a4

High performance InAlN/GaN high electron mobility transistors for low voltage applications

Minhan Mi(宓珉瀚), Meng Zhang(张濛), Sheng Wu(武盛), Ling Yang(杨凌), Bin Hou(侯斌), Yuwei Zhou(周雨威), Lixin Guo(郭立新), Xiaohua Ma(马晓华), Yue Hao(郝跃)
Chin. Phys. B . 2020, 29(5): 057307 . **doi:** 10.1088/1674-1056/ab821e

Quantum fluctuation of entanglement for accelerated two-level detectors

Si-Xuan Zhang(张思轩), Tong-Hua Liu(刘统华), Shuo Cao(曹硕), Yu-Ting Liu(刘宇婷), Shuai-Bo Geng(耿率博), Yu-Jie Lian(连禹杰)
Chin. Phys. B . 2020, 29(5): 050402 . **doi:** 10.1088/1674-1056/ab7d9a

Effect of AlGaN interlayer on luminous efficiency and reliability of GaN-based green LEDs on silicon substrate

Jiao-Xin Guo(郭娇欣), Jie Ding(丁杰), Chun-Lan Mo(莫春兰), Chang-Da Zheng(郑畅达), Shuan Pan(潘拴), Feng-Yi Jiang(江风益)
Chin. Phys. B . 2020, 29(4): 047303 . **doi:** 10.1088/1674-1056/ab7903

Fabrication and performance evaluation of GaN thermal neutron detectors with ^{6}LiF conversion layer*

Zhifu Zhu(朱志甫)[1,2,3], Zhijia Sun(孙志嘉)[2,†], Jijun Zou(邹继军)[3,‡], Bin Tang(唐彬)[2], Qinglei Xiu(修青磊)[2], Renbo Wang(王仁波)[3], Jinhui Qu(瞿金辉)[3], Wenjuan Deng(邓文娟)[3], Shaotang Wang(王少堂)[3], Junbo Peng(彭俊波)[3], Zhidong Wang(王志栋)[3], Bin Tang(汤彬)[3], and Haiping Zhang(张海平)[4]

[1] *State Key Laboratory Breeding Base of Nuclear Resources and Environment, East China University of Technology, Nanchang* 330013, *China*
[2] *State Key Laboratory of Particle Detection and Electronics, Institute of High Energy Physics, Chinese Academy of Sciences, Beijing* 100049, *China*
[3] *Engineering Research Center of Nuclear Technology Application (East China University of Technology), Ministry of Education, Nanchang* 330013, *China*
[4] *CGN Begood Technology Co., Ltd., Nanchang* 330013, *China*

(Received 3 May 2020; revised manuscript received 25 May 2020; accepted manuscript online 12 June 2020)

A GaN-based pin neutron detector with a ^{6}LiF conversion layer was fabricated, and can be used to detect thermal neutrons. Measurement of the electrical characteristic of the GaN-based pin neutron detector showed that the reverse leakage current of the neutron detector was reduced significantly after deposition of a ^{6}LiF conversion layer on the detector surface. The thermal neutrons used in this experiment were obtained from an ^{241}Am–Be fast neutron source after being moderated by 100-mm-thick high-density polyethylene. The experimental results show that the detector with 16.9-μm thick ^{6}LiF achieved a maximum neutron detection efficiency of 1.9% at a reverse bias of 0 V, which is less than the theoretical detection efficiency of 4.1% calculated for our GaN neutron detectors.

Keywords: thermal neutron, GaN, detector, ^{6}LiF

PACS: 04.80.Nn, 29.40.–n, 73.40.Kp, 73.61.Ey **DOI:** 10.1088/1674-1056/ab9c05

1. Introduction

As a direct wide-band-gap semiconductor material, gallium nitride (GaN) is considered to be the most suitable semiconductor material to prepare high-power, high-temperature, and high-frequency electronic devices because of its high saturated electron-drift velocity, high thermal conductivity, high breakdown electric field, large band gap, and favorable chemical stability.[1] In recent years, GaN has been studied extensively as a radiation-detection material because of its large bandgap and high threshold-displacement energy.[2–4] GaN is a good candidates to application in high-temperature and high-radiation fields, such as neutron logging and high-energy physics experiments.[5–7] The preparation of GaN-based radiation detectors, including x-ray, α-particle, and β-particle has been achieved using different epitaxial growth and doping technologies, substrate materials, and device structures.[8] Device performance measurements for α-particle detection indicated that the charge collection efficiency (CCE) was close to 100% under a reverse bias range from -2 V to 20 V.[9] In order to achieve neutron detection, GaN-coated neutron conversion materials on its surface, such as ^{6}LiF or $^{10}B_4C$, can also be modified into a neutron detector. Melton *et al.*[10] grew 10-μm thick Si-doped GaN on sapphire substrates, and fabricated GaN-based neutron scintillator by coating neutron conversion material ^{6}LiF. Their experimental results show that the pulse height spectrum with 2.05-MeV alpha particle was observed in thermal neutron scintillation spectra produced by the ^{241}Am–Be, and moderated to thermal energy by a graphite pile. Wang *et al.*[11] reported their results fabricated in a sandwich Schottky structure detector using a freestanding n-type GaN, using a Li_2O enriched with 7.5% ^{6}Li isotope as a neutron moderating layer and a polytetrafluoroethylene (PTFE) as a moderator to detect fast neutrons, obtained energy peak of triton with 2.73 MeV and alpha particles with 2.055 MeV. Although GaN-based neutron detectors have been studied, more detailed fabrication processes and performance measurements have not been reported by the ^{6}LiF conversion layer for thermal neutron detection.

In this work, a GaN-based pin neutron detector was prepared by coating the neutron conversion layer with ^{6}LiF. The electrical properties of the pre- and post-coated ^{6}LiF detectors were investigated from I–V measurements. The α-particle detection properties with a pre-coating of ^{6}LiF were evaluated by an incident 5.48-MeV ^{241}Am source at room temperature. A thermal neutron detection using a detector with a 100-mm-

*Project supported by the National Natural Science Foundation of China (Grant Nos. 61964001 and 61961001), the State Key Laboratory of Particle Detection and Electronics (Grant No. SKLPDE-KF-2019), the Natural Science Foundation of Jiangxi Province, China (Grant Nos. 20192BAB207033 and 20181BAB202026), the Foundation of State Key Laboratory Breeding Base of Nuclear Resources and Environment (East China Institute of Technology) (Grant No. NRE1515), and the Jiangxi Provincial Postdoctoral Science Foundation, China (Grant No. 2018KY31).

†Corresponding author. E-mail: sunzj@ihep.ac.cn
‡Corresponding author. E-mail: jjzou@ecit.cn

© 2020 Chinese Physical Society and IOP Publishing Ltd

thick polyethylene (PE) moderator and 16.9-μm thick ^{6}LiF conversion layer was achieved with an ^{241}Am–Be fast neutron source. The main purpose of this work is to investigate the thermal neutron detection characteristics of the GaN-based pin detector with ^{6}LiF grown on sapphire substrates.

2. Experimental details

2.1. Principle of thermal neutron detection

Fast neutrons are moderated through a high-density hydrogen-rich PE moderator material to thermal neutrons. The thermal neutrons react with ^{10}B and ^{6}Li conversion material to produce charged particles, and the charged particles cause ionization in the detector.

By using a nuclear reaction method, the ^{10}B and ^{6}Li conversion materials are coated on the front of the detector to detect charged particles. Although the thermal neutron absorption cross section for ^{6}Li is lower than that with ^{10}B in the conversion material, the higher reaction product energies make it attractive for thermal neutron detection. The neutron conversion mechanism is based on the well-known nuclear reaction equation for ^{6}Li:

$$^{6}\mathrm{Li} + \mathrm{n} \rightarrow \alpha(2.05\ \mathrm{MeV}) + \mathrm{T}(2.73\ \mathrm{MeV}), \quad Q = 4.78\ \mathrm{MeV}. \tag{1}$$

In equation (1), 2.05-MeV alpha particles and 2.73-MeV tritons that are produced in the thermal neutron reaction on ^{6}Li are emitted in opposite directions.

2.2. Sample preparation

GaN epilayers were grown on *c*-plane Al_2O_3 substrates using a metal–organic chemical–vapor–deposition (MOCVD) system with a 3 × 2-in (1 in = 2.54 cm) aixtron close-coupled showerhead growth chamber, which is used extensively in the materials growth of the most III–nitride-based commercial high-power LEDs. The GaN-based pin device structure is composed of Si-doped n-GaN, unintentionally doped i-GaN, and Mg-doped p-GaN with thicknesses of 2, 5, and 0.3 μm, respectively. The carrier concentrations of n-GaN, i-GaN, and p-GaN that were obtained from Hall measurements at room temperature were 8×10^{18}, 1.2×10^{17}, and 1.6×10^{17} cm^{-3}, respectively. According to the semi-empirical formula, the dislocation density of the GaN pin film is calculated from the x-ray rocking curve to be $\sim 4 \times 10^{8}$ cm^{-2}.[12] The mesa-structure GaN-based pin detector with a 1-mm diameter was fabricated by inductively-coupled plasma with $Cl_2/BCl_3/Ar$ etching down to the n-GaN layer. Ti/Al/Ni/Au (20/50/20/300 nm) ohmic contact metallizations on n-GaN were prepared by an electron-beam evaporator and alloyed at 550 ℃ for 900 s in nitrogen by rapid thermal annealing, followed by deposition Ni/Au (20 nm/300 nm) ohmic contact on p-GaN and annealing at 500 ℃ for 900 s in air by rapid thermal annealing.[13] After the ohmic contact had been prepared, the device was bound to an Au-plated printed circuit board using an ultrasonic wire bonding with a 25-μm-diameter Au wire. The GaN-based pin neutron detector was prepared by evaporating ^{6}LiF powder enriched with 16.9-μm-thick 95% ^{6}Li isotope on the entire device surface by thermal evaporation in vacuum. The device structure with evaporated ^{6}LiF is shown in Fig. 1(a). Finally, nine neutron detectors mounted in the PCB with Au-plated contact by 25-μm-thick gold wires, as shown in Fig. 1(b).

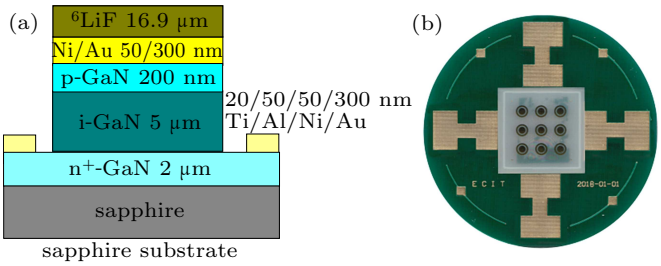


Fig. 1. (a) Device structure evaporated ^{6}LiF; (b) photograph of nine neutron detectors mounted in the PCB with Au-plated contact by 25-μm gold wires. External ring contact (Ti/Al/Ni/Au) and internal circular contact (Ni/Au) were connected to the VCC and GND of the applied voltage, respectively. The dimensions in the picture are not drawn to scale.

2.3. Experimental assembly

The thermal neutrons used in this experiment were obtained from an ^{241}Am–Be fast neutron source (4.08-MeV mean neutron energy) after being moderated by 100-mm-thick high-density polyethylene, which is a metal cylinder with a bottom diameter of 15 mm and a height of 20 mm, and the fast neutron flux was close to 2.2×10^{4} cm^{-2}·s^{-1}. The neutron activity of the ^{241}Am–Be neutron source used in our experiment is provided by the company producing the isotope element, which is about 2×10^{5} Bq and belongs to the category V exempt source. Figure 2 shows the neutron detection system diagram using an ORTEC modular pulse-processing electronic analyzer. We simulated the moderating efficiency of fast neutrons as a function of PE thickness. The simulation results show that the highest fast neutron slowdown efficiency can be achieved when the PE thickness is 100 mm. The PE with a 150-mm diameter and a thickness of 30 mm was excavated along the center of the 25-mm-diameter circle with a depth of 20 mm, and the ^{241}Am–Be fast neutron source was embedded in the PE groove. A second PE with a 150-mm diameter and a thickness of 100 mm was used to moderate fast neutrons into thermal neutrons. The distance L1 between the detector and the moderator PE was less than 5 mm, and the distance L2 of the moderator PE from the neutron source was less than 1 mm. To reduce the influence of external light sources, electromagnetic waves, and background noise on the measuring results, the detector, moderator PE, and neutron source were placed in a stainless-steel container and sealed. The GaN-based neutron detection experiment was carried out at room temperature.

The electrical characteristics of the devices before and after ^{6}LiF evaporation were analyzed from the *I–V* characteristics. The thermal neutron detection apparatus were connected to a standard ORTEC modular pulse-processing electronic analyzer, as shown in Fig. 2, which is consisted of a charge-sensitive pre-amplifier 142PC, an ORTEC model 428 detector bias, a shaper amplifier 572A with a shaping time of 1 μs, and a pulse-counting board. The pulse-counting board was developed in-house and consisted of a voltage comparator with adjustable threshold voltages, square waveform shaper, counter, and display module. Moderated thermal neutrons were irradiated towards the detector surface with a ^{6}LiF converter.

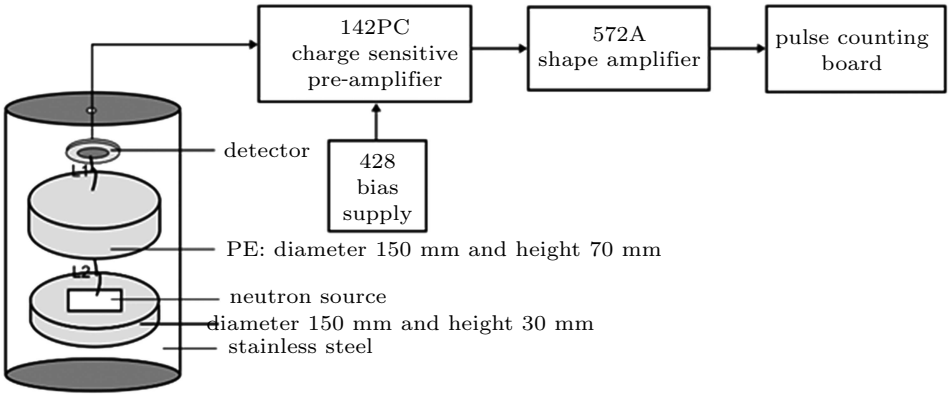


Fig. 2. Neutron detection-system diagram using ORTEC modular pulse-processing electronic analyzer.

2.4. Simulation

We simulate the thermal neutron capture yield produced by fast neutrons captured with PE as a function of the thicknesses using GENT4, as shown in Fig. 3. According to an GENT4 simulation for PE, the optimum PE thickness is about 10 cm.

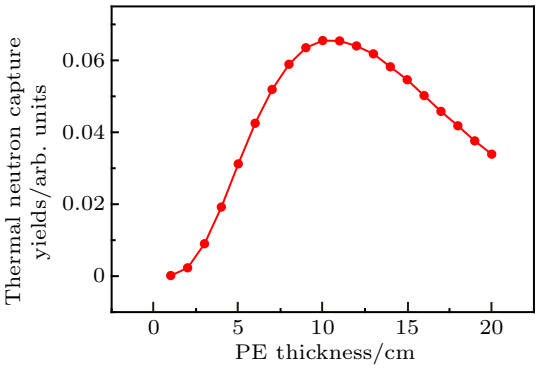


Fig. 3. The thermal neutron capture yield produced by fast neutrons captured with PE as a function of the thicknesses using GENT4.

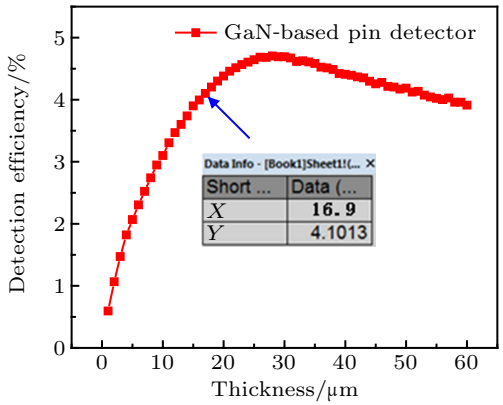


Fig. 4. Thermal neutron detection efficiency as a function of the ^{6}LiF converter thickness.

We also used GENT4 to simulate the relationship between the neutron detection efficiency of our detector and the converter thickness, as shown in Fig. 4. The plot shows that the detection efficiency starts to saturate with a converter thickness around 26 μm. The inner graph is an indication of the detection efficiency of ^{6}LiF with a thickness of 16.9 μm.

3. Results and discussion

3.1. Current–voltage characteristics measurements

Figure 5 shows the reverse bias *I–V* characteristic curves of the pin detectors before and after deposition of the ^{6}LiF conversion layer. The leakage currents of the neutron detector before and after ^{6}LiF deposition that were obtained from the *I–V* curves for a reverse bias of 60 V were 151 nA and 41 nA, respectively. The reverse leakage current of the detector after ^{6}LiF deposition was reduced significantly. For planar devices, silicon dioxide is often used as a surface-passivation

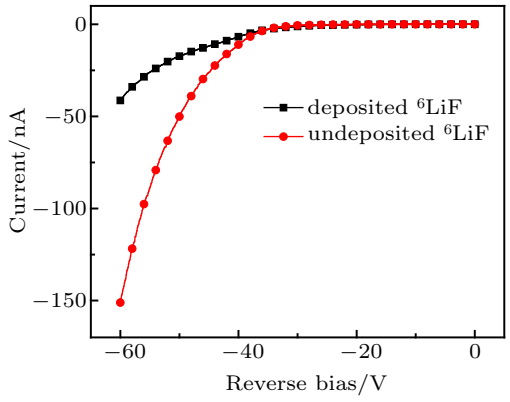


Fig. 5. The *I–V* characteristics of neutron detectors before and after deposition of ^{6}LiF under various reverse bias voltages.

layer to prevent sodium and potassium ions from migrating through the oxide, which reduces the leakage current of the device. ^{6}LiF is an insulator medium for a neutron conversion material, and is similar to silicon-dioxide passivation, which reduces the leakage current on the device surface after deposition. Similar features have been found for GaAs neutron detectors with a ^{6}LiF conversion layer.[14]

3.2. Alpha detection

The neutron detection based on the nuclear reaction method is still the detection of charged particles. Prior to the detection of neutrons, we measured the alpha-particle spectrum of the device. Figure 6 shows the pulse height spectrum of ^{241}Am under different reverse bias voltages. The total count of the energy spectrum is the highest under a reverse bias of 0 V, and the total count decreases as the reverse bias voltage increases. This result shows that the device has good characteristics for detecting charged particles before ^{6}LiF vapor deposition.

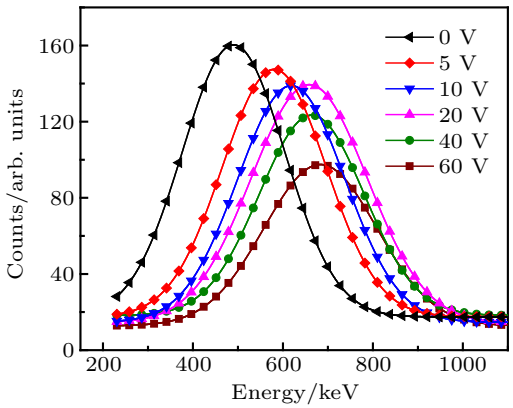


Fig. 6. Pulse-height spectrum of neutron detector irradiated by 5.48-MeV ^{241}Am alpha particles as a function of reverse bias voltages at room temperature.

3.3. Neutron detection

When ^{241}Am–Be emits neutrons, it also emits gamma rays. In order to shield the effects of gamma rays on the detector, ^{241}Am–Be was placed in a lead-shielded can with a thickness of 50 mm. Before test detector was exposed to ^{241}Am–Be, the ^{241}Am–Be was first placed in a closed lead can with a thickness of 50 mm to shield the gamma rays emitted by ^{241}Am–Be. Secondly, the neutron detector measures the effect of the background on the detector count at 2 h, and the display count of the pulse-counting board is 0 at a threshold voltage of 50 mV. Six groups of pulse counts of neutron detector under different reverse bias voltages and different threshold voltages are listed in Table 1.

At different reverse bias voltages, the neutron detector leakage current is not the same, and the noise level after system amplification is also different. Therefore, when the pulse counts of the neutron detectors under different reverse bias voltages are measured, the threshold voltage of the pulse-counting board needs to be adjusted to deduce the effect of noise level on the neutron pulse count and to distinguish the pulse voltage signal produced by charged particles in GaN from the neutron source irradiation after ^{6}LiF conversion. As listed in Table 1, a GaN neutron detector for thermal neutron detection has been achieved by coating with a 16.9-μm-thick ^{6}LiF conversion layer. The maximum total counts of the detector was achieved at a reverse bias of 0 V, and reached 168, and then the total counts decreased with an increase in bias voltage, which may be attributed to the increasing detector noise under a higher reverse bias voltage.

The detection efficiency is an important parameter of the neutron detector. The detection efficiency of the neutron detector, η, is defined as the ratio of neutron number detected by detectors to the total number of emissions from the neutron source during the measurement time. η is expressed as

$$\eta = \frac{N_{\mathrm{D}} \times S_{\mathrm{D}}}{n \times S_{\mathrm{n}} \times t}, \tag{2}$$

where N_{D} is the measured number of counts recorded by the neutron detector from the pulse-counting board, n is the neutron flux (neutron/s), t is the measurement time in seconds and S_{D} and S_{n} are the effective area of the detector and the area of the neutron source in unit cm^2, respectively.

Table 1. Pulse counts of neutron detector from pulse-counting board under different biases voltages.

Voltage/V	Pulse counts (t = 1 h)						Total counts	Threshold voltage/mV
	1	2	3	4	5	6		
0	24	31	27	31	28	27	168	50
5	20	26	22	32	32	24	156	100
10	19	28	20	33	21	29	150	150

In this neutron detection experiment, the ^{241}Am–Be neutron source has an emission angle of 2π relative to the detector. By combining Table 1 and Eq. (2), we estimate the detection efficiency of our detector for thermal neutron. The detection efficiency with ^{6}LiF and a conversion-layer thickness of 16.9 μm was 1.90%, 1.76%, and 1.70% for a reverse bias of 0 V, 5 V, and 10 V, respectively, which is lower than the theoretical detection efficiency of 4.1% calculated for our GaN neutron detectors. The experimental results indicated that this is due to the poor quality of the GaN crystals grown by

MOCVD. The defect density of hetero-epitaxially grown GaN is higher than 10^5 cm^{-3}. It is possible to grow thicker unintentionally doped GaN epitaxially to achieve wide SCR for the detection of alpha-particles, but high background carrier concentrations for GaN are still a major challenge. In addition, it may also be due to the fact that no collimator is used in the measurement. Polyakov *et al.*[15] prepared a GaN Schottky diode grown on sapphire by the MOCVD epitaxial lateral overgrowth technique, and 75% enriched ^{10}B isotope was deposited on top of the Schottky diodes with a 10-μm thickness by spraying from alcohol solution, spinning the layer on a centrifuge spinner, and protecting it with epoxy. The estimated neutron detection efficiency was $\sim 0.5\%$ in their experiment. The thermal detection efficiency of our detector is higher than their experimental values because of the larger depletion region width of our detector and the higher purity of ^{6}LiF isotopes in the conversion layer.

4. Conclusions

GaN-based pin neutron detectors with ^{6}LiF conversion layers were fabricated to detect thremal neutrons that were emitted from an ^{241}Am–Be fast-neutron source moderated by a high-density PE moderator. The electrical characteristics measurement results of the neutron detector shown that the reverse leakage current of the neutron detector was reduced significantly because mobile ions on the surface and edges of the device that deposited a ^{6}LiF conversion layer were passivated. The maximum thermal neutron detection efficiency of the detector with a ^{6}LiF thickness of 16.9 μm was estimated to be approximately 1.9% at a reverse bias voltage of 0 V. When a bias voltage is applied across the detector, although the electric field of the device increases, the leakage current of the device increases. After the neutron is irradiated on the detector, it is affected by factors such as structures, material thickness, and conversion efficiency. The electron hole pairs generated by the ray in the device and the electrical signals induced at both ends of the electrode are relatively small, and part of the signal is submerged in the electron noise, this part of the signal does not contribute to the efficiency of neutron detection. When no bias is applied across the device electrodes, because our GaN device structure has a very strong built-in electric field sufficient to partially deplete the device, there is no electronic noise in the detector, and the electrical signal after radiation is greater than the noise. Therefore, the device has the highest neutron detection efficiency at zero bias. To improve the detection efficiency of the GaN neutron detector, more work is required to optimize the ^{6}LiF thickness and the structure of the detector.

References

[1] Shur M S 1998 *Solid State Electron.* **42** 2131
[2] Wu Y F, Keller B P, Keller S, Kapolnek D, Kozodoy P, Denbaars S P and Mishra U K 1996 *Appl. Phys. Lett.* **69** 1438
[3] Asif Khan M, Kuznia J N, Olson D T, Schaff W J, Burm J W and Shur M S 1994 *Appl. Phys. Lett.* **65** 1121
[4] Nakamura S, Mukai T and Senoh M 1994 *Appl. Phys. Lett.* **64** 1687
[5] Northrup J E and Neugebauer J 1996 *Phys. Rev. B* **53** R10477
[6] Zhu Z F, Zou J J, Tang B, Wang Z D, Peng X C, Liang H W, Zhang H Q and Du G T 2018 *Nucl. Instrum. Method A* **902** 9
[7] Zhu Z F, Zhang H Q, Liang H W, Tang B, Peng X C, Liu J X, Yang C, Xia X C, Tao P C, Shen R S, Zou J J and Du G T 2018 *Nucl. Instrum. Method A* **893** 39
[8] Taheri A and Sheidaiy M 2015 *J. Inst.* **10** 05003
[9] Geng X L, Xia X C, Huang H L, Sun Z H, Zhang H Q, Cui X Z, Liang X H and Liang H W 2020 *Chin. Phys. B* **29** 027201
[10] Melton A G, Burgett E, Xu T, Hertel N and Ferguson I T 2012 *Phys. Status Solidi* **9** 957
[11] Wang J H, Mulligan P, Brillson L and Cao L R 2015 *Appl. Phys. Rev.* **2** 031102
[12] Li Y, Shi Z F, Li X J and Shan C X 2019 *Chin. Phys. B* **28** 017803
[13] Wang W F, Wang J F, Zhang Y M, Li T K, Xiong R and Xu K 2020 *Chin. Phys. B* **29** 047305
[14] Šagátová A, Zatko B, Sedlackova K, Necas V, Dubecky F, Bohacek P and Chodak I 2013 *Nucl. Instrum. Method A* **8** 03016
[15] Polyakov A Y, Smirnov N B, Shchemerov I V, Gogova D, Tarelkin S A, Lee I H and Pearton S J 2018 *ECS. J. Solid State Sci.* **7** 260